Technical Paper

ISSN 1996-6814 Int. J. Pavement Res. Technol. 6(5):520-526

Evaluating the Influence of Aggregate Size on Permeability of Porous Pavements Using Finite Volume Simulation

Lei Zhang[1], Ghim Ping Ong[1+], and Tien Fang Fwa[1]

Abstract: Porous pavement is widely used to enhance wet weather skid resistance on highways through its superior drainage capacity. Porosity within the porous pavement structure typically serves as the control variable during the design and construction phases, while permeability is the functional parameter indicating drainage performance during the operation phase. One potential implication of using porosity during design and construction and permeability during operations is that porous pavement layer pore structures resulting from different aggregate sizes can result in different permeability values despite having identical porosity values. Recognizing this issue, this paper first presents a theoretical analysis on the drainage capacity of porous pavement. Outflow tests on typical porous pavements with various aggregate sizes are then simulated using the finite volume method and simulation results are validated against experimental measurements. It is concluded from our study that aggregate size has a significant influence on the permeability of porous pavement and should be included during pavement design, construction and operations.

DOI:10.6135/ijprt.org.tw/2013.6(5).520
***Key words**: Aggregate size; Finite volume model; Permeability; Porous pavement.*

Introduction

Wet-weather road safety is a major concern of road users and pavement engineers. Hydroplaning and insufficiency of skid resistance are two of the most dangerous situations a vehicle may encounter when rain water is accumulated on pavement surface. Specially designed with higher air void content, porous pavement is identified as an excellent engineering countermeasure to the reduction of skid resistance on wet pavement. The Association of Japan Highway reported an 80% reduction in accidents on wet pavements when porous surfaces were used [1]. The enhancement of wet pavement skid resistance brought forth by porous pavements is highly dependent on the drainage capacity within the porous layer. For a porous pavement with better drainage properties, water can be effectively dispelled from tire-pavement contact area and resulting in greater tire-pavement contact and hence better friction. Drainage in the porous pavement layer is achieved through an interconnected pore network which serves as drainage channels to relieve hydrodynamic pressure developed underneath the tire when a vehicle travels on a wet pavement surface.

Two indicators are commonly used in practice to evaluate the drainage capacity of a porous pavement layer. Porosity is a measure on the amount of voids within the layer, and permeability is a measure on the ability of the porous layer to allow water to pass through it. Porosity is often accepted as a convenient volumetric parameter in asphalt or concrete mixture design, because it can be efficiently measured and controlled. Although drainage capacity is directly related to the fraction of connected air void within pavement material, it is inadequate to predict porous pavement permeability using porosity as the sole parameter [2-4]. One reason is that aggregate shape and size can significantly affect the size of pores and the tortuosity of capillaries, all of which are influential in porous pavement drainage performance. To date, studies on porous pavement permeability are mainly experimental in nature and there are few research studies exploring the influence of aggregate size on pavement permeability numerically.

This paper therefore approaches this problem from a theoretical-numerical perspective. After a brief overview of associated literature on measurement and modelling of porous pavement permeability, the flow condition within a porous layer under specific pressure conditions is analysed theoretically. A numerical model is then developed using the finite volume method to simulate the outflow meter experiments. Simulations on porous pavement layers with similar porosity values but different aggregate sizes are next performed and the influence of aggregate size on pavement permeability is analyzed numerically.

Literature Review

Constant-head and falling-head outflow meters are typically adopted to measure pavement permeability both in field and in laboratory. These test methods were first standardized in geotechnical engineering [5] and is then widely accepted in pavement engineering [6]. Jones and Jones [7] developed a constant-head device to measure permeability of compacted aggregates. Permeability of porous medium was found to be dependent on the hydraulic gradient in a constant-head test. Tan et al. [8, 9] developed a falling-head apparatus to measure the permeability of porous asphalt. The permeability obtained from this permeameter was found to be in close agreement with that from a constant head test. It was also found from their studies that void content alone is inadequate to describe the drainage property of porous asphalt. Neithalath et al. [10] conducted falling-head permeability measurements on pervious concretes, and found that permeabilities

[1] Department of Civil and Environmental Engineering, National University of Singapore.
[+] Corresponding Author: E-mail ceeongr@nus.edu.sg
Note: Submitted January 15, 2013; Revised May 23, 2013; Accepted May 24, 2013.

differed by more than 100% for concrete specimens with similar porosities. From the numerous past experimental studies [2-4, 10-14], it was concluded that while in general permeability is related to porosity, representing permeability as a function of porosity alone is inadequate and can be misleading. Pore size distribution, tortuosity of capillaries and pore connectivity have significant influences on the drainage properties of porous pavements.

Besides past experimental studies which aimed at developing a relationship between permeability and pore structure parameters, previous research studies also attempted to model flow within porous pavements numerically. Jackson and Ragan [15] described the hydraulic behaviour of porous pavement parking lots with the assumption of Darcy's flow and provided numerical solutions to the Boussinesq equation. Adler et al. [16] solved the Stokes equation of a Newtonian fluid in fictitious porous media by a finite difference scheme. Finite element method is adopted by Chuai [2] to study the flow properties through porous slabs. Bordier and Zimmer [17] developed an analytical solution of Boussinesq equation with Izbash's law by a semi-analytical approach, which was used in water table prediction. Ranieri [18] developed a model to simulate the runoff on porous pavements, considering road geometry, rainfall intensity and pavement permeability. Solutions to the analytical hydraulic equations governing flow in porous pavements were presented by Charbeneau and Barrett [19] where steady state Darcy flow and Dupuit-Forchheimer assumptions were applied.

Besides formulating the macroscopic flow condition within porous media, the microstructure of the pore network was also modelled. The effect of pore size distribution on saturated permeability was studied by Wise [20] using a conceptual cubic network model with cylindrical capillary tubes. Liang et al. [21] characterized geometric parameters of porous medium based on morphological skeletonization. The skeleton was derived by a fully parallel thinning algorithm and topological analysis. A three-dimensional pore network model was developed by Acharya et al. [22] where the locations and sizes of pore throats were determined by power functions of Beti's influence lines. Fractal theory was adopted by Yu et al. [23] to model the permeability of fractal porous medium and derive the pore size probability. Kuang et al. [24] generated the microstructure parameters from X-ray tomography and examined hydraulic conductivity of permeable pavements with a series of pore-structure models. X-ray tomography technique was also adopted by Masad et al. [25] and Gruber et al. [26] to rebuild the microstructure of porous asphalt, and simulate the flow field. Zhang et al. [27] proposed an iterative process based on a grid pore structure to model the outflow tests, and predict the drainage capacity of porous pavements. Random-sequential adsorption approach was used by Umiliaco and Benedetto [14] to generate pore structure from randomly extracted spherical particles, and Lattice-Boltzmann method was used to solve the unsteady flow within these pores.

From the existing literature, it is clear that the influence of aggregate size on permeability of porous pavement has drawn great interest among to pavement researchers. Due to the difficulties in design and control of pore-network structure in practice, experiments cannot fully reveal the mechanisms, nor answer the question quantitatively. Numerical models of flow within microstructure of porous media have the potential to cover this gap, however few publications on this particular topic are available to date. Therefore, this paper analyzes the influence of aggregate size of a porous pavement on its permeability numerically, using a simple structural pore-network model which is proved capable in the drainage capacity simulation of porous pavement.

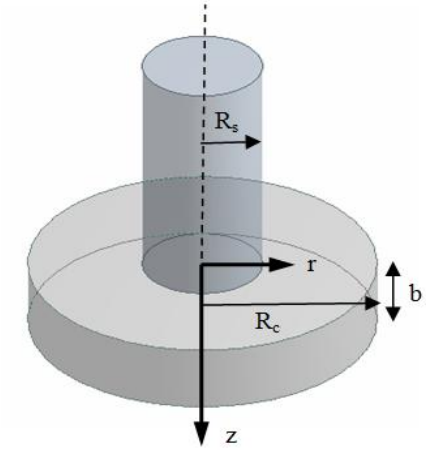

Fig. 1. Porous Specimen in Cylindrical Coordinates.

Methodology

The theories and methods used in the numerical simulation is presented in this section. Permeability of a porous specimen is first derived under the assumptions of both Darcy and non-Darcy flows. The equivalence between constant-head test and falling-head test is also demonstrated. This theory is next applied in the finite volume model simulating the constant-head outflow tests on porous pavements. Computational fluid dynamics theories considered in the numerical model are briefly described. Air voids within porous pavement are represented by a simplified pore network and aggregate size is modeled using variations in pore size and spacing. The outflow results obtained from simulation model are then validated against experimental measurements.

Permeability Computation

The concepts of permeability and hydraulic conductivity are sometimes misused without distinction. Permeability is a measure of the ability of a porous material to allow fluids to pass through it, while hydraulic conductivity is a property of material that describes the ease with which water can move through pore spaces. The relationship between permeability (κ) and hydraulic conductivity (k) is

$$\kappa = k\frac{\mu}{\rho g} \tag{1}$$

where μ = fluid dynamic viscosity, ρ = fluid density, and g = acceleration due to gravity. Hydraulic conductivity is also named as permeability coefficient. In practice, it is more convenient to measure hydraulic conductivity through a constant-head or falling-head test and then convert the result to permeability through Eq. (1).

Three-dimensional hydraulic conductivity for Darcy flow can be derived from the steady-state continuity equation [28]. For an isotropic porous specimen located in cylindrical coordinates (Fig. 1), the continuity equation is

$$\frac{1}{r}\frac{\partial}{\partial r}\left(r\frac{\partial h}{\partial r}\right)+\frac{\partial^2 h}{\partial z^2}=0 \tag{2}$$

with the boundary conditions:

$$h(r,z)=h_s(t) \qquad [0\le r\le R_s; z=0] \tag{3}$$

$$h(r,z)=0 \qquad [r=R_c; 0\le z\le b_c] \tag{4}$$

$$\frac{\partial h(r,z)}{\partial z}=0 \qquad [R_s<r\le R_c; z=0] \tag{5}$$

$$\frac{\partial h(r,z)}{\partial z}=0 \qquad [0\le r\le R_c; z=b_c] \tag{6}$$

If both R_c and b_c are infinite, the solution is given as

$$h(r,z)=\frac{2}{\pi}h_s\, sin^{-1}\left(\frac{2R_s}{\sqrt{(r-R_s)^2+z^2}+\sqrt{(r+R_s)^2+z^2}}\right) \tag{7}$$

It is related to discharge through

$$Q=-2\pi k\int_0^{R_s} r\frac{\partial h(r,0)}{\partial z}dr=4kh_sR_s \tag{8}$$

Therefore, the isotropic hydraulic conductivity k can then be computed as

$$k=\frac{Q}{4h_sR_sF}. \tag{9}$$

where F is a shape factor addressing the effect of finite specimen dimensions.

To take account of the nonlinear effect in non-Darcy flow, a heuristic correlation can be made and the following relationship is proposed [2]:

$$v=ki^m \tag{10}$$

where k is the pseudo hydraulic conductivity, and m is the flow condition index (value in range of 0.5 to 1). An m value of 1 indicates a fully laminar flow while an m value of 0.5 represents a fully turbulent flow. Apply the natural logarithmic

$$ln(v)=ln(k)+m\,ln(i) \tag{11}$$

For a falling-head test, the variation of hydraulic head with time can be approximated with a cubic function [28]:

$$h=a_0+a_1t+a_2t^2+a_3t^3. \tag{12}$$

The mean velocity can computed by differentiating Eq. (12) with respect to time:

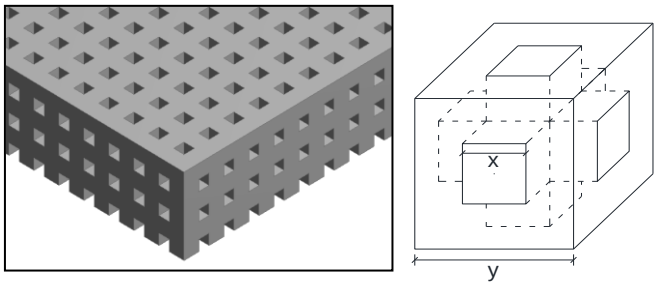

(a) Geometry of porous pavement layer (b) Cubic pore element

Fig. 2. Pore Network Structure of Porous Pavement Model.

$$v=\frac{dh}{dt}=a_1+a_2t+a_3t^2 \tag{13}$$

Noting that $i = h / l$ (l = thickness of porous specimen), values of v and i can then be derived from test data at different times ***t***. Using Eq. (11), permeability k can be obtained through regression. For a constant-head test, flow rate Q can be measured at different hydraulic gradients i and the mean velocity v is easily derived from flow rate Q and cross-section area A.

Model Geometry

A grid pore-network model has been developed by the authors in their previous work [27]. This model is proved to be computationally efficient for permeability modelling applications. Connected air voids within porous pavements are simplified as straight channels in all the longitudinal, transverse and vertical directions (Fig. 2), with a cubic pore element spatially repeated in the three directions. Two variables are needed to specify this structure, namely the edge length of each drainage channel as denoted by x, and the distance between centres of two successive parallel channels as denoted by y. The size of a single drainage channel is an indicator of the representative pore size in the porous pavement layer, and the spacing of successive channels is related to the nominal aggregate size in the porous mixture with single-size aggregates. The sizes of pores and aggregates in actual pavements can be characterized by stereological or mathematical morphology based methods [10, 28].

An iterative process was developed to calibrate the model. Details of this process can be found in the authors' previous work [27]. A nominal porosity ϕ_0 can be obtained from the mix design, and a minimum x value is set to prevent the model to be numerically oversize. The convergence criterion is a sufficiently small residual between numerical and experimental results, typically 5%.

CFD Consideration

Water flow in porous pavement layer is close to turbulence rather than laminar. Therefore, k-ε turbulence model is used to account for the turbulence effects. It relates Reynolds stresses to mean velocity gradient and turbulent viscosity by gradient diffusion hypothesis. The continuity and momentum equations are defined as:

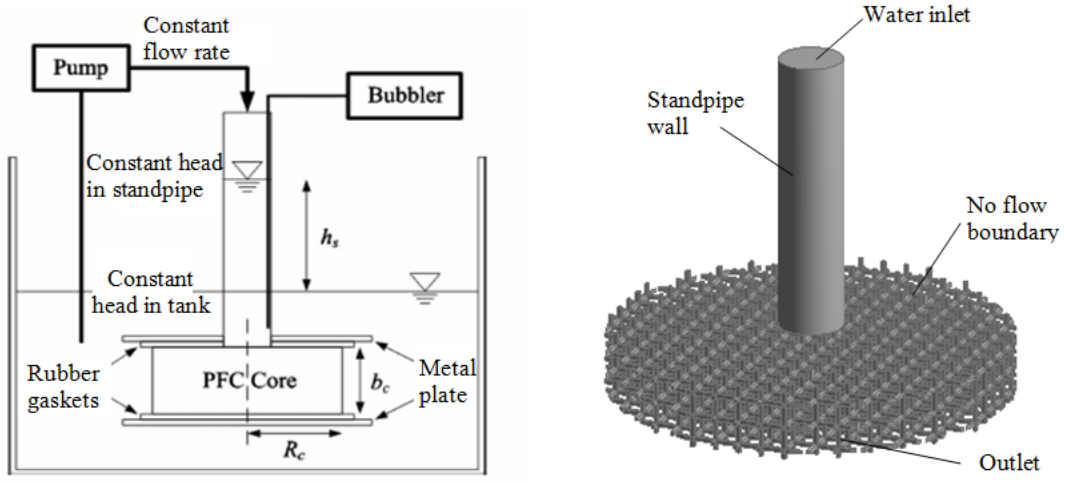

Fig. 3. Illustrated Device and Model of Constant-head Permeability Test.

$$\frac{\partial \rho}{\partial t} + \nabla(\rho U) = 0 \tag{14}$$

$$\frac{\partial \rho U}{\partial t} + \nabla(\rho U \otimes U) = -\nabla p' + \nabla\left(\mu_{eff}\left(\nabla U + (\nabla U)^T\right)\right) + S_M \tag{15}$$

where S_M = sum of body forces, p' = modified pressure = $P + \frac{2}{3}\rho k + \frac{2}{3}\mu_{eff}\nabla U$, and μ_{eff} = effective viscosity = $\mu + \mu_t$. The turbulence viscosity μ_t is calculated by:

$$\mu_t = C_\mu \rho \frac{k^2}{\varepsilon} \tag{16}$$

where k = turbulence kinetic energy, ε = turbulence eddy dissipation, and C_μ = constant. The values of k and ε come directly from the differential transport equations:

$$\frac{\partial(\rho k)}{\partial t} + \nabla(\rho U k) = \nabla\left[\left(\mu + \frac{\mu_t}{\sigma_k}\right)\nabla k\right] + P_k + P_{kb} - \rho\varepsilon \tag{17}$$

$$\frac{\partial(\rho \varepsilon)}{\partial t} + \nabla(\rho U \varepsilon) = \nabla\left[\left(\mu + \frac{\mu_t}{\sigma_\varepsilon}\right)\nabla \varepsilon\right] + \frac{\varepsilon}{k}\left(C_{\varepsilon 1}\left(P_k + P_{\varepsilon b}\right) - C_{\varepsilon 2}\rho\varepsilon\right) \tag{18}$$

where $C_{\varepsilon 1}$, $C_{\varepsilon 2}$, σ_k and σ_ε are constants, P_{kb} and $P_{\varepsilon b}$ represent buoyancy turbulence, and P_k is the turbulence production due to viscous forces.

Model Validation

The proposed model has been validated against past experimental data. The one illustrated here is the constant-head experiment conducted by Charbeneau et al. [29]. The sketches of the test apparatus and model setup are shown in Fig. 3. Simulation conditions are specified based on actual experimental conditions. Fig. 4 compares the outflow result obtained from simulation model with that from experiments, and a good agreement can be observed.

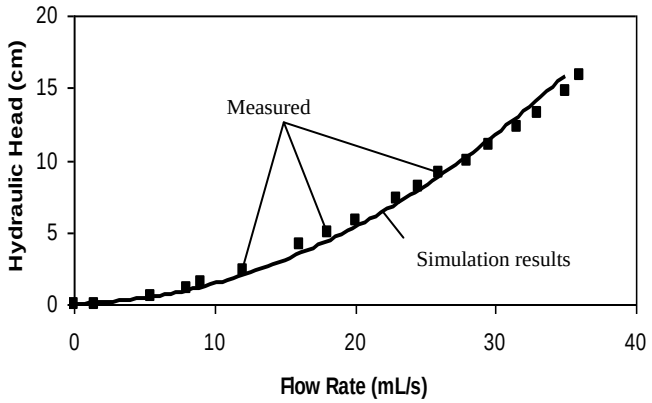

Fig. 4. Comparison between Numerical and Experimental Results of Charbeneau et al. Test [29].

Results and Discussion

Although porous pavement is commonly designed with single-size aggregates, it is not realistic for an actual mixture to be made up by aggregates with identical size and shape. Moreover, pore sizes and capillaries are never uniformly distributed within the mixture. X-ray tomography is widely used in experimental studies to identify the pore network structure within a porous mixture specimen [24-26], however this method needs special technique and it is very difficult to artificially control the pore size in experiments. Therefore, a simplified representation of porous surface layer structure is adopted in this paper (Fig. 5) to transform the actual pore structure to a grid network as shown in Fig. 2. It is derived that, for a specific porosity value ϕ_0, the ratio between pore size x and aggregate size y is a constant. If set $x/y = c$, the relationship is

$$\phi_0 = \frac{V_{pore}}{V_{total}} = \frac{3x^2 y - x^3}{y^3} = c^2(3 - c) \tag{19}$$

Porous mixtures with three porosity levels (15%, 20% and 25%) and four aggregate sizes (8mm, 12mm, 16mm and 20mm) are

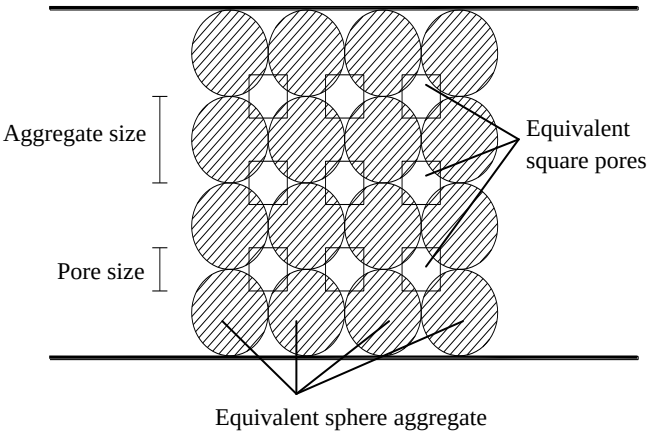

Fig. 5. Simplified Representation of Porous Layer Structure.

Table 1. Geometry Parameters in Simulated Cases.

Porosity [%]	$c = x/y$	Aggregate Size [mm]	Pore Size [mm]
15	0.233	8	1.86
		12	2.80
		16	3.73
		20	4.66
20	0.271	8	2.17
		12	3.25
		16	4.34
		20	5.42
25	0.305	8	2.44
		12	3.66
		16	4.88
		20	6.10

examined in this case study. The geometry parameters corresponding to each case are listed in Table 1. All the simulations are conducted on 100 mm thick porous layers and the diameter of outflow meter is 150 mm. The influence of outflow meter dimensions (60 mm, 90 mm, 120 mm and 150 mm) on the simulation results is also examined on a specimen with 20% porosity and 12 mm aggregate size.

Simulations of constant-head outflow tests are conducted under five hydraulic heads (200 mm, 300 mm, 400 mm, 500 mm and 600 mm) for each mixture type. The mass flow rate is monitored as the direct output of the model. Fig. 6 illustrates the simulation results of 20% porosity mixture and similar curves are obtained for mixtures with porosities of 15% and 25%. The permeability values are next derived from the direct model outputs. Specific velocity is easily derived from flow rate, and hydraulic gradient is taken as the ratio between hydraulic head and specimen thickness. Eq. (11) is then used in liner regression to calculate hydraulic conductivity, and permeability is derived by Eq. (1). The calculation results of all the mixture types are shown in Fig. 7.

As expected, the permeability of porous pavement increases with the increase of porosity. It is more important to see from Fig. 7 that aggregate size has a significant influence on permeability of porous pavement despite having the same porosity value. A larger aggregate

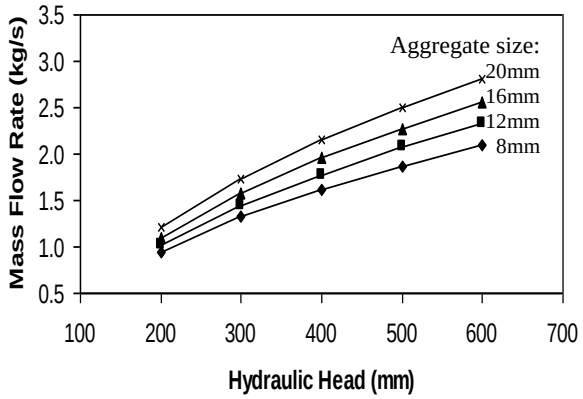

Fig. 6. Simulation Results of Constant-head Outflow Tests on Porous Pavement with 20% Porosity.

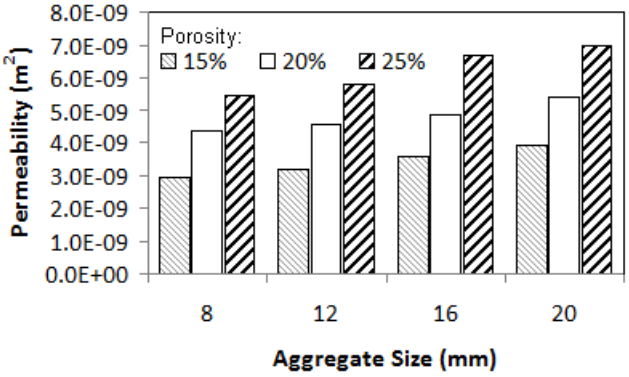

Fig. 7. Influence of Porosity and Aggregate Size on Permeability Value.

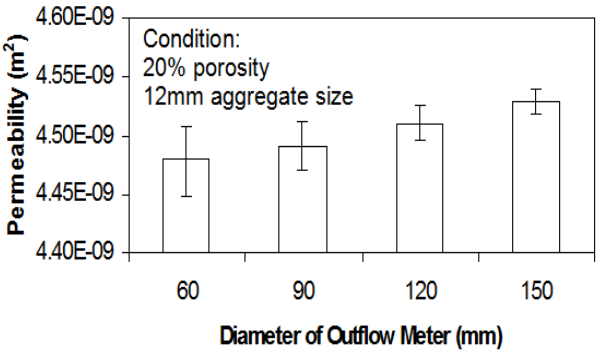

Fig. 8. Influence of Outflow Meter Diameter on Simulated Permeability Value.

size tends to produce a higher permeability value. This may be a result of having a lower orifice perimeter and higher hydraulic radius. This observation means that when design pavement mix and during construction, designers should account for the potential effect of aggregate size on porosity and permeability.

It was also found from the simulations that the speed of the water being discharged into the porous pavement layer is related to the outflow meter diameter and the relative position the outflow meter is allocated (Fig. 8). It was found from the analyses that the larger the outflow diameter is, the smaller variance it provides during the

tests. Therefore, a larger outflow diameter (and hence a larger outflow area) and a higher number of measurement points extracted during the outflow test can greatly enhance the reliability of outflow test on porous pavement. Quantitative analyses on this problem could be conducted in the future work.

Conclusion and Recommendation

The complicated pore structure of porous pavement is simplified by a grid network model, the drainage capacity of which is numerically equivalent to that of actual porous pavements. With proper calibration and validation, this model is used to analyze the influence of aggregate size on porous pavement permeability. Three porosity levels and four aggregate sizes are examined numerically through the simulation of constant-head outflow tests. It is concluded from the simulation results that aggregate size has a significant influence on permeability, despite the same porosity being maintained. Pores formed by larger aggregates have higher hydraulic radius. They are easier for water to pass through, thus have a higher permeability. It is inadequate to consider porosity as the sole functional parameters representing the drainage capacity in the design and construction processes of porous pavements. It is necessary to control the aggregate size and directly measure permeability in laboratory and in field to understand the drainage performance of a particular compacted porous mixture. In the other conditions being equal, larger-size aggregates are recommended in porous mixture design to provide better drainage performance for the completed pavement. The influence of aggregate size on permeability may also affect the skid resistance performance of porous pavements with identical porosity. Such effects could be investigated in the future with a similar approach as presented in this work.

References

1. Association of Japan Highway (1996). Guide for Porous Asphalt Pavement. Maruzen Corporation, Tokyo, Japan.
2. Chuai, C.T. (1998). Measurement of Drainage Properties of Porous Asphalt Mixtures, Ph.D. thesis, National University of Singapore, Singapore.
3. Liu, Q. and Cao, D. (2009). Research on material composition and performance of porous asphalt pavement, *Journal of Materials in Civil Engineering*, 21, pp. 135-140.
4. Kuang, X., Sansalone, J., Ying, G., and Ranieri, V. (2011). Pore-structure model of hydraulic conductivity for permeable pavement, *Journal of Hydrology*, 399, pp. 148-157.
5. ASTM (2006). Standard test method for permeability of granular soils (constant head), ASTM Standard D2434-68, American Society for Testing and Materials, Pennsylvania.
6. ASTM (2009). Standard test method for measuring pavement texture drainage using an outflow meter, ASTM Standard E2380-09, American Society for Testing and Materials, Pennsylvania.
7. Jones, H.A. and Jones, R.H. (1989). Horizontal permeability of compacted aggregates, *Proceedings of 3rd Symposium on Unbound Aggregates in Roads*, pp. 70-77.
8. Tan, S.A., Fwa, T.F., and Cuai, C.T. (1997). New apparatus for measuring the drainage properties of porous asphalt mixes, Journal of Testing and Evaluation 25 (1997) 370-377.
9. Tan, S.A., Fwa, T.F., and Chuai, C.T. (1999). Automatic field permeameter for drainage properties of porous asphalt mixes, *Journal of Testing and Evaluation*, 27, pp. 57-62.
10. Neithalath, N., Sumanasooriya, M.S., and Deo, O. (2010). Characterizing pore volume, size, and connectivity in pervious concretes for permeability prediction, *Materials Characterization*, 61, pp. 802-812.
11. Bhutta, M.A.R., Tsuruta, K., and Mirza, J. (2012). Evaluation of high-performance porous concrete properties, *Construction and Building Materials*, 31, pp. 67-73.
12. Huang, B., Wu, H., Shu, X. and Burdette, G. (2010). Laboratory evaluation of permeability and strength of polymer-modified pervious concrete, *Construction and Building Materials*, 24, pp. 818-823.
13. Kayhanian, M., Anderson, D., Harvey, J.T., Jones, D., and Muhunthan, B. (2012). Permeability measurement and scan imaging to assess clogging of pervious concrete pavements in parking lots, *Journal of Environmental Management*, 95, pp. 114-123.
14. Umiliaco, A. and Benedetto, A. (2012). Unsteady flow simulation of water drainage in open-graded asphalt mixtures, *Procedia - Social and Behavioral Sciences*, 53, pp. 346-355.
15. Jackson, T.P. and Ragan, R.M. (1974). Hydrology of porous pavement parking lots, *Journal of the Hydraulics Division*, 100, pp. 1739-1752.
16. Adler, P.M., Jacquin, C.G., and Quiblier, J.A. (1990). Flow in simulated porous media, *International Journal of Multiphase Flow*, 16, pp. 691-712.
17. Bordier, C. and Zimmer, D. (2000). Drainage equations and non-Darcian modelling in coarse porous media or geosynthetic materials, *Journal of Hydrology*, 228, pp. 174-187.
18. Ranieri, V. (2002). Runoff control in porous pavements, *Transportation Research Record*, No. 1789, pp. 46-55.
19. Charbeneau, R.J. and Barrett, M.E. (2008). Drainage hydraulics of permeable friction courses, *Water Resources Research* (on line, W04417, doi:10.1029/2007WR006002).
20. Aise, W.R. (1992). A new insight on pore structure and permeability, *Water Resources Research*, 28, pp. 189-198.
21. Liang, Z., Ioannidis, A., and Chatzis, I. (2000). Geometric and topological analysis of three-dimensional porous media: pore space partitioning based on morphological skeletonization, *Journal of Colloid and Interface Science*, 221, pp. 13-24.
22. Acharya, R.C., van der Zee, S., and Leijnse, A. (2004). Porosity-permeability properties generated with a new 2-parameter 3D hydraulic pore-network model for consolidated and unconsolidated porous media, *Advances in Water Resources*, 27, pp. 707-723.
23. Yu, B., Zoy, M., and Feng, Y. (2005). Permeability of fractal porous media by Monte Carlo simulations, *International Journal of Heat and Mass Transfer*, 48, pp. 2787-2794.
24. Kuang, X., Sansalone, J., Ying, G., and Ranieri, V. (2011). Pore-structure model of hydraulic conductivity for permeable pavement, *Journal of Hydrology*, 399, pp. 148-157.
25. Masad, E., Omari, A.A., and Chen, H.C. (2007). Computations of permeability tensor coefficients and

anisotropy of asphalt concrete based on microstructure simulation of fluid flow, *Computational Materials Science*, 40, pp. 449-459.

26. Gruber, I., Zinovik, I., Holzer, L., Flisch, A., and Poulikakos, L.D. (2012). A computational study of the effect of structural anisotropy of porous asphalt on hydraulic conductivity, *Construction and Building Materials*, 36, pp. 66-77.
27. Zhang, L., Ong, G.P., and Fwa, T.F. (2012). Three dimensional modeling of porous pavement permeability using a simplified pore network structure, *Proceedings of the 7th International Conference on Maintenance and Rehabilitation of Pavements and Technological Control*, Auckland, New Zealand.
28. Sumanasooriya, MS. And Neithalath, N. (2009). Stereology and morphology based pore structure descriptors of enhance porosity (pervious) concretes, *Materials Journal*, 106, pp. 429-438.
29. Charbeneau, R.J., Klenzendorf, L.B., and Barrett, M.E. (2011). Methodology for determining laboratory and in situ hydraulic conductivity of asphalt permeable friction course, *Journal of Hydraulic Engineering*, 137, pp. 15-22.